Physica A 508 (2018) 595–607

Contents lists available at ScienceDirect

Physica A

journal homepage: www.elsevier.com/locate/physa

Weighted multivariate composite multiscale sample entropy analysis for the complexity of nonlinear times series

Ningning Zhang [a], Aijing Lin [a,*], Hui Ma [b], Pengjian Shang [a], Pengbo Yang [a]

[a] School of Science, Beijing Jiaotong University, Beijing 100044, PR China
[b] Beijing Raysdate Company Limited, Beijing 100102, PR China

HIGHLIGHTS

- We propose the weighted multivariate composite multiscale sample entropy (WMMCSE) in order to measure the complexity of nonlinear time series.
- And WMCMSE overcomes inaccurate results as the coarse-graining procedure reduces the length of the time series at a large scale and inability to detect abrupt changes in the signal and ignore the difference between distinct patterns of multivariate multiscale sample entropy (MMSE).
- Compared with the multivariate multiscale sample entropy (MMSE), weighted multivariate multiscale sample entropy (WMMSE), multivariate composite multiscale sample entropy (MCMSE), WMCMSE is more sensitive to parameters and the changes of the values of WMCMSE are steadier on random series.
- Beijing has a large population and the complicated traffic situation, and the behaviors of Ring 2, 3, 4 road at different times are also different.

ARTICLE INFO

Article history:
Received 29 August 2017
Received in revised form 1 March 2018
Available online 31 May 2018

Keywords:
Multivariate multiscale sample entropy (MMSE)
Weighted multivariate multiscale sample entropy (WMMSE)
Multivariate composite multiscale sample entropy (MCMSE)
Weighted multivariate composite multiscale sample entropy (WMCMSE)
Complexity
Traffic time series

ABSTRACT

Multivariate multiscale sample entropy (MMSE) has recently been proposed to evaluate complexity of time series. However, the results of estimation of complexity by MMSE method may be inaccurate as the coarse-graining procedure reduces the length of the time series at a large scale. In addition, MMSE has some limitations, mainly its inability to detect abrupt changes in the signal and ignore the difference between distinct patterns. In order to overcome those above limitations of MMSE, this paper introduces the weighted multivariate composite multiscale sample entropy (WMCMSE) as a measure to characterize the complexity of nonlinear time series. And we illustrate the necessity of WMCMSE method by comparing WMCMSE results with multivariate multiscale sample entropy (MMSE), weighted multivariate multiscale sample entropy (WMMSE), multivariate composite multiscale sample entropy (MCMSE) on random series. Then, WMCMSE method is employed to study the complexity of traffic speed and volume time series of Beijing Ring 2, 3, 4 roads, which are from August 11th to October 20th, 2012. The results of WMCMSE show that the WMCMSE method can distinguish the behavior of the flow time series, which means that we can detect the congested traffic system. We found that road condition of ring 2, 3, 4 road is very different. Compared to the ring 4 road, the values of the WMCMSE of the ring 2 and 3 roads are higher, indicating that the traffic flow on Ring 2 and Ring 3 road are more complex compared to Ring 4 road. The higher the complexity, the more traffic jams. Government departments can judge the traffic congestion of that time period and that road

* Corresponding author.
E-mail address: ajlin@bjtu.edu.cn (A. Lin).

https://doi.org/10.1016/j.physa.2018.05.085
0378-4371/© 2018 Published by Elsevier B.V.

according to the complexity differences between different time periods and different roads, and then take different measures.

© 2018 Published by Elsevier B.V.

1. Introduction

Complexity in nonlinear time series is an intrinsic feature of dynamical systems [1–5]. Entropy measures that quantify the complexity of the time series have attracted growing interests because these measures depend on the underlying dynamics/function of the system. When the underlying dynamics or kinetics of system changes, the complexity of the time series will reflect such changes, which might not be able to detect by traditional statistical measures. However, the study on the complexity of real data, such as traffic series, is regulated by some factors such as its environment or mechanism [6–10]. The complexity of the traffic time series has attracted intense interest [11–17], and various methods are developed to estimate the complexity of the traffic signals [18,19], e.g., multiscale sample entropy (MSE). In 2002, Costa et al. [20] proposed the multiscale entropy (MSE) which has been applied in many fields successfully [21–23]. The MSE algorithm calculates sample entropy (SampEn) over a range of scales to represent the complexity of a time series. However, as a complexity measurement, there is a strong limitation in the MSE methodology [24,25]. It is specifically designed for analyzing univariate time series, thus restricting the complexity analysis of multivariate time series, and does not consider couplings, long term correlation and causality. In 2012, the multivariate multiscale entropy (MMSE) [24] was proposed to evaluate the complexity in multiple data channels over different time scales, and it deals with the different embedding dimensions, time lags, and amplitudes [26–30].

Although MMSE is able to uncover the underlying multivariate dynamical complexity and the long-range correlations of traffic time series, it may yield an inaccurate estimation of entropy or induce undefined entropy because of the coarse-graining procedure reducing the length of a time series [31–33]. The larger the scale factor, the shorter the coarse-grained time series [34]. In order to overcome these drawbacks, we herein introduce the multivariate composite multiscale entropy algorithms (MCMSE) to address the accuracy concern of the MMSE algorithm [32]. In the MCMSE algorithm, at a scale factor of ϵ, the sample entropies of all coarse-grained time series, corresponding to different starting points of the coarse-graining process, are calculated and the MCMSE value is defined as the means of ϵ entropy values. Compared with the MMSE method, the MCMSE is used to estimate entropy more accurately. However, considering that MCMSE does not take the effect of noise into account and weights it uniformly, we propose the weighted multivariate composite multiscale entropy algorithms (WMCMSE) to solve this problem [35–39]. WMCMSE has the advantages of detecting abrupt changes in the signal. WMCMSE also performs better when applied to signals containing amplitude-coded information because of its immunity to degradation by noise and (linear) distortion. The weighted approach makes it possible to detect the abrupt changes in the data and assigns more weight to the regular spiky patterns [40]. In other words, it is clearly able to differentiate between small fluctuations (may due to effect of noise) and large fluctuations of time series.

In this paper, we prove the validity of WMCMSE method by comparing it with traditional analysis methods such as MMSE, MCMSE, WMMSE. The experimental results show that WMCMSE is superior to the other three methods. Mainly, our analysis is based on the traffic speed and volume time series, which are from different detectors of Beijing Ring 2, 3, 4 roads from August 11th to October 20th, 2012. The Ring 2 road is closer to the city center, followed by the Ring 3 road, the Ring 4 road finally. They are all in the city, just different partitions. The findings presented in this paper are helpful for understanding the traffic system and also reflect the traffic congestion.

The structure of this paper is organized as follows. We briefly introduce MSE, MMSE, WMMSE, MCMSE, WMCMSE algorithms in Section 2. Section 3 lists the data used in our work, including random series and traffic data of Beijing and is devoted to validating the effectiveness of the new proposed method by comparing it with MMSE, MCMSE, WMMSE on random series. In Section 4 we provide the detailed complexity analysis of WMCMSE on traffic volume and speed time series. Finally, a conclusion is presented in Section 4.

2. Methodology

2.1. Original multiscale sample entropy (MSE)

The original multiscale sample entropy (MSE) is proposed by Costa [20,22] as an effective complexity measure for time series over different time scales. For a one-dimensional time series $\{x_i\}_{i=1}^{N}$ of length N, MSE first constructs multiple coarse-grained time series. The coarse-grained procedure is performed by averaging the data points inside the consecutive but non-overlapping window of increasing scale factor ϵ. Thus, the coarse-grained time series of $\{x_i\}_{i=1}^{N}$ can be calculated as

$$y_j^{(\epsilon)} = \frac{1}{\epsilon} \Sigma_{i=(j-1)\epsilon+1}^{j\epsilon} x_i \tag{1}$$

where $1 \leq j \leq N/\epsilon$. For scale $\epsilon = 1$, the coarse-grained time series $\{y^{(1)}\}$ corresponds to the original time series. The length of the coarse-grained time series $\{y^{(\epsilon)}\}$ is N/ϵ.

The next step is computation of the sample entropy for each new reconstructed coarse-grained signals $\{y^{(\epsilon)}\}$ with scale factor ϵ. Computation of sample entropy is performed as follows:

(1) Form the $N/\epsilon - m + 1$ vectors $y_m^{(\epsilon)}(i)$ as

$$\begin{aligned} &y_m^{(\epsilon)}(i) = [y^{(\epsilon)}(i), y^{(\epsilon)}(i+1), \ldots, y^{(\epsilon)}(i+m-1)], \\ &i = 1, \ldots, N/\epsilon - m + 1 \end{aligned} \tag{2}$$

where m is the length of sequences to be compared.

(2) The maximum norm $d_m[y_m^{(\epsilon)}(i), y_m^{(\epsilon)}(j)]$ between two such vectors is computed as

$$\begin{aligned} &d_m[y_m^{(\epsilon)}(i), y_m^{(\epsilon)}(j)] = max[|\, y_m^{(\epsilon)}(i+k) - y_m^{(\epsilon)}(j+k)\,|], \\ &0 \leq k \leq m-1 \end{aligned} \tag{3}$$

(3) Define the function

$$\begin{aligned} &B_i^m(r) = \frac{1}{N/\epsilon - m + 1} u^m(i), \\ &i = 1, \ldots, N/\epsilon - m + 1 \end{aligned} \tag{4}$$

where r is the tolerance for accepting matrices, and u^m is the number of $d_m[y_m^{(\epsilon)}(i), y_m^{(\epsilon)}(j)] \leq r$, for $i \neq j$

(4) Define the function

$$\begin{aligned} &A_i^m(r) = \frac{1}{N/\epsilon - m + 1} v^{m+1}(i), \\ &i = 1, \ldots, N/\epsilon - m + 1 \end{aligned} \tag{5}$$

where v^{m+1} is the number of $d_{m+1}[y_{m+1}^{(\epsilon)}(i), y_{m+1}^{(\epsilon)}(j)] \leq r$, for $i \neq j$

(5) Then, we calculate the probability of matching points,

$$B^m(r) = \frac{1}{N/\epsilon - m + 1} \sum_{i=1}^{N/\epsilon - m + 1} B_i^m(r) \tag{6}$$

$$A^m(r) = \frac{1}{N/\epsilon - m} \sum_{i=1}^{N/\epsilon - m} A_i^m(r) \tag{7}$$

where $B^m(r)$ and $A^m(r)$ respectively represent the probability that two sequences will match for m and $m+1$ points.

(6) The theoretical value of the sample entropy is defined as

$$SampEn(m, r) = \lim_{N/\epsilon \longrightarrow \infty} \{-\ln \frac{A^m(r)}{B^m(r)}\} \tag{8}$$

For a finite length of data points N/ϵ, the estimate of the sample entropy is given by

$$SampEn(m, r, N) = -\ln[\frac{A^m(r)}{B^m(r)}] \tag{9}$$

2.2. Multivariate multiscale sample entropy (MMSE)

Similarly, for the algorithm of MMSE, the number of channels should be taken into account. Given the multivariate time series $\{x_{k,i}\}_{i=1}^N$, $k = 1, 2, \ldots, p$, where p denotes the number of variables (channels) and N the number of samples in each variate. The multivariate multiscale sample entropy(MMSE) analysis is performed through the following steps:

(1) Construct the multivariate coarse-grained time series $\{y_{k,j}^{(\epsilon)}\}$ as

$$y_{k,j}^{(\epsilon)} = \frac{1}{\epsilon} \Sigma_{i=(j-1)\epsilon+1}^{j\epsilon} x_{k,i} \tag{10}$$

where $1 \leq k \leq p$, $1 \leq i \leq N$, and $1 \leq j \leq N/\epsilon$.

(2) Form $(N/\epsilon - n)$ composite delay vectors $Y_m^{(\epsilon)}(j) \in R^m$ for each coarse grained multivariate time series $y_{k,j}^{(\epsilon)}$ which can be expressed as follows,

$$\begin{aligned} &Y_m^{(\epsilon)}(j) = [y_{1,j}^{(\epsilon)}, y_{1,j+\tau_1}^{(\epsilon)}, \ldots, y_{1,j+(m_1-1)\tau_1}^{(\epsilon)}, y_{2,j}^{(\epsilon)}, y_{2,j+\tau_2}^{(\epsilon)}, \\ &\ldots, y_{2,j+(m_2-1)\tau_2}^{(\epsilon)}, y_{p,j}^{(\epsilon)}, y_{p,j+\tau_p}^{(\epsilon)}, \ldots, y_{p,j+(m_p-1)\tau_p}^{(\epsilon)}] \end{aligned} \tag{11}$$

where $m = \sum_{k=1}^{p} m_k$, $M = [m_1, m_2, \ldots, m_p] \in R^p$ is the embedding vector, $\tau = [\tau_1, \tau_2, \ldots, \tau_p]$ the time lag vector, $j = 1, 2, \ldots, N/\epsilon - n$ and $n = max\{M - 1\} \times max\{\tau\}$.

(3) Define the distance between any two vectors $Y_m^{(\epsilon)}(j)$ and $Y_m^{(\epsilon)}(l)$ as the maximum norm, that is,

$$d[Y_m^{(\epsilon)}(j), Y_m^{(\epsilon)}(l)] = max_{h=1,2,\ldots,m}\{|\, y^{(\epsilon)}(j+h-1) - y^{(\epsilon)}(l+h-1)\,|\} \tag{12}$$

Calculate sample entropy for each coarse-grained multivariate $\{y_{k,j}^{(\epsilon)}\}$.

(4) For a given composite delay vector $Y_m^{(\epsilon)}(j)$ and a threshold r, count the number of instances Q_j where $d[Y_m^{(\epsilon)}(j), Y_m^{(\epsilon)}(l)] \le r, j \ne l$. Then we calculate the frequency of occurrence $B_j^m(r) = \frac{1}{N/\epsilon-n-1} Q_j$, and define a global quantity

$$B^m = \frac{1}{N/\epsilon - n} \sum_{j=1}^{N/\epsilon-n} B_j^m(r) \tag{13}$$

(5) We extend the dimension of composite delay vectors from m to $m+1$ and form the $Y_{m+1}^{(\epsilon)}(j)$. This can be performed in p different ways in which we can evolve from the space of dimension m described by the embedding vector $M = [m_1, m_2, \ldots, m_p] \in R^p$ to any space of dimension for which the embedding vector is $m_1, m_2, \ldots, m_p$ where $k = 1, 2, \ldots, p$ is the number of data channel. Thus, a total of $p \times (N/\epsilon - n)$ vectors $Y_{m+1}^{(\epsilon)}(j)$ in R^{m+1} can be obtained, where $Y_{m+1}(\epsilon)(j)$ is any embedded vector upon increasing the embedding dimension from m_k to $(m_k + 1)$ for a specific variable k.

(6) For a given $Y_{m+1}^{(\epsilon)}(j)$, calculate the number of vectors Q_j, where $d[Y_{m+1}^{(\epsilon)}(j), Y_{m+1}^{(\epsilon)}(l)] \le r, j \ne l$, then calculate the frequency of occurrence $B_j^{m+1}(r) = \frac{1}{p(N/\epsilon-n)-1} Q_j$, and define the global quantity

$$B^{m+1}(r) = \frac{1}{p(N/\epsilon - n)} \sum_{j=1}^{p(N/\epsilon-n)} B_j^{m+1}(r) \tag{14}$$

(7) Finally, for a tolerance level r, estimate as MMSE for each coarse-grained multivariate time series $\{y_{k,j}^{(\epsilon)}\}$ as

$$MMSE(x, M, \epsilon, r, N) = -\ln[\frac{B^{m+1}(r)}{B^m(r)}] \tag{15}$$

2.3. Weighted multivariate multiscale sample entropy (WMMSE)

The weighted multivariate multiscale sample entropy (WMMSE) we propose is based on multivariate multiscale sample entropy to quantify complexity of multivariate signals across different time scales.

(1) For a given composite delay vector $y_j^{(\epsilon)}$, we define the weight value w_j is the variance of each vector $y_j^{(\epsilon)}$

$$w_j = \frac{1}{m}[\sum_{s=1}^{p}\sum_{k=1}^{m_k}(y_{(1,j+(k-1)\epsilon_s)} - \bar{Y}_m^{(\epsilon)}(j))] \tag{16}$$

For a given threshold r, we find all the vectors that satisfy this equation $d[Y_m^{(\epsilon)}(j), Y_m^{(\epsilon)}(l)] \le r, j \ne l$. Then, we calculate the frequency of occurrence $B_j^m(r) = \frac{\sum_{l:d[Y_m^{(\epsilon)}(j), Y_m^{(\epsilon)}(l)]\le r} w_l}{\sum_{i\le N/\epsilon-n, i\ne j} w_i}$, and define a global quantity

$$B^m = \frac{\sum_{j=1}^{N/\epsilon-n} B_j^m(r)}{\sum_{i\le N/\epsilon-n} w_i} \tag{17}$$

(2) Similarly, for the sequence $Y_{m+1}^{(\epsilon)}(j)$, we can get the

$$\begin{aligned} B_j^{m+1}(r) &= \frac{\sum_{l:d[Y_{m+1}^{(\epsilon)}(j), Y_{m+1}^{(\epsilon)}(l)]\le r} w_l}{\sum_{i\le N/\epsilon-n, i\ne j} w_i} \\ B^{m+1} &= \frac{\sum_{j=1}^{N/\epsilon-n} B_j^{m+1}(r)}{\sum_{i\le N/\epsilon-n} w_i} \end{aligned} \tag{18}$$

(3) Finally, for a tolerance level r, estimate as WMMSE for each coarse-grained multivariate time series $y_{k,j}^{(\epsilon)}$ as

$$WMMSE(x, W, M, \epsilon, r, N) = -\ln[\frac{B^{m+1}(r)}{B^m(r)}] \tag{19}$$

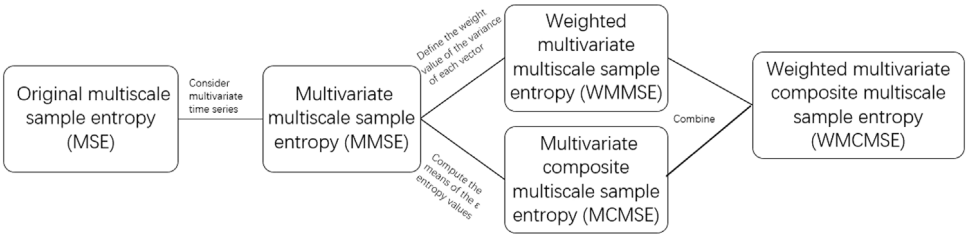

Fig. 1. The relations among original multiscale sample entropy (MSE), multivariate multiscale sample entropy (MMSE), weighted multivariate multiscale sample entropy (WMMSE), multivariate composite multiscale sample entropy (MCMSE) and weighted multivariate composite multiscale sample entropy (WMCMSE).

2.4. Multivariate composite multiscale sample entropy (MCMSE)

Consider a time series $(x_i, 1 \le i \le N)$. *MSE* is computed as follows. First, the original signal is divided into non-overlapping segments of length ϵ. Second, a selected moment is estimated for the data in each of these segments to derive the coarse-grained time series at scale ϵ. Here, we focus solely on the second moment using an unbiased estimator $\sigma^2 = 1/(N-1)\sum_{i=1}^{N}(x_i - x)^2$ of variance. Third, a measure of entropy, sample entropy [41], is calculated for each coarse-grained time series. Fourth, a complexity index is derived by adding the entropy values for a selected range of scales.

In order to reduce the variance of estimated entropy values at large scales, Wu et al. [34] proposed the composite multiscale entropy. For a discrete time series $x = x_1, \ldots, x_i, \ldots, x_N$, the kth coarse-gained time series for a scale factor ϵ is defined as $y_k^{(\epsilon)} = y_{k,1}^{(\epsilon)}, y_{k,2}^{(\epsilon)}, \ldots, y_{k,p}^{(\epsilon)}$, where $y_{k,j}^{(\epsilon)} = \frac{1}{\epsilon}\sum_{i=(j-1)\tau+k}^{j\tau+k-1} x_i$, $1 \le j \le \frac{N}{\epsilon}$, $1 \le k \le \epsilon$. Then, at a sale factor ϵ the sample entropy values of all coarse-grained time series are computed and the *CMSE* is defined as the means of the ϵ entropy values $CMSE(x, \epsilon, m, r) = \frac{1}{\epsilon}\sum_{k=1}^{\epsilon}(-\ln \frac{n_{k,\epsilon}^{m+1}}{n_{k,\epsilon}^{m}})$.

The multivariate composite multiscale sample entropy(MCMSE) is performed through the following steps:

(1) For an p-dimensional time series $\{x_{k,i}\}_{i=1}^{N}$, $k = 1, 2, \ldots, p$, construct the coarse-grained time series $y_{k,j}^{(\epsilon)}$ according to Eq. (10).
(2) In the MCMSE algorithm, at a scale factor of ϵ, calculate the SampEns of all coarse-grained time series and the MCMSE value is defined as the means of ϵ SampEns; that is:

$$\begin{aligned} MCMSE(x, M, \epsilon, m, r) &= \frac{1}{\epsilon}\sum_{k=1}^{\epsilon} MMSE(y_k^{(\epsilon)}, M, \epsilon, r, N) \\ &= \frac{1}{\epsilon}\sum_{k=1}^{\epsilon}(-\ln \frac{n_{k,\epsilon}^{m+1}}{n_{k,\epsilon}^{m}}) \end{aligned} \tag{20}$$

where $n_{k,\epsilon}^{m}$ represents the total number of m-dimensional matched vector pairs and is constructed from the kth coarse-grained time series at a scale factor of ϵ.

2.5. Weighted multivariate composite multiscale sample entropy (WMCMSE)

The weighted multivariate composite multiscale sample entropy (WMCMSE) is performed through the following steps:

(1) For an p-dimensional time series $\{x_{k,i}\}_{i=1}^{N}$, construct the coarse-grained time series $y_{k,j}^{(\epsilon)}$ according to Eq. (10).
(2) In the WMCMSE algorithm, at a scale factor of ϵ, calculate the SampEns of all coarse-grained time series and the WMCMSE value is defined as the means of ϵ SampEns; that is:

$$\begin{aligned} WMCMSE(x, \epsilon, m, r) &= \frac{1}{\epsilon}\sum_{k=1}^{\epsilon} WMMSE(y_k^{(\epsilon)}, \\ &\quad W, N, \epsilon, r, N) \\ &= \frac{1}{\epsilon}\sum_{k=1}^{\epsilon}(-\ln \frac{n_{k,\epsilon}^{m+1}}{n_{k,\epsilon}^{m}}) \end{aligned} \tag{21}$$

where $n_{k,\epsilon}^{m}$ denotes the total number of m-dimensional matched vector pairs and is constructed from the kth coarse-grained time series at a scale factor of ϵ.

More specifically, we show the relations between all these methods introduced in Section 2 (see Fig. 1).

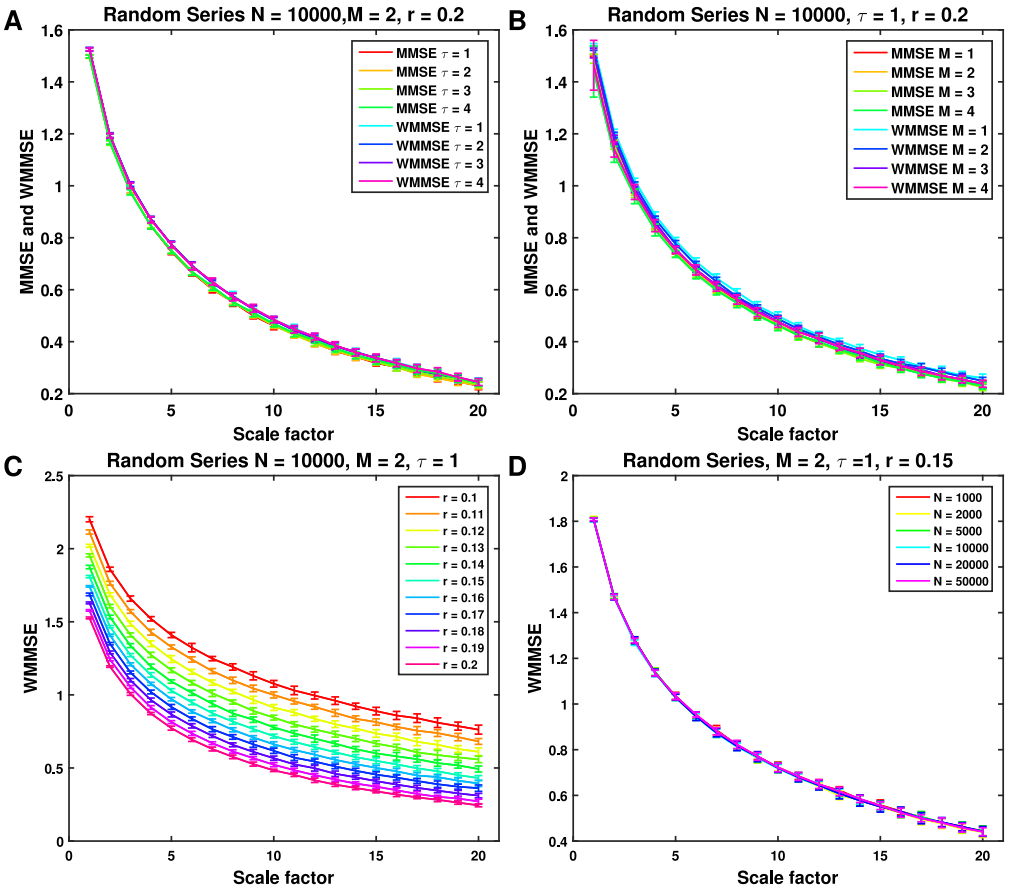

Fig. 2. Applying the multivariate multiscale sample entropy (MMSE) and weighted multivariate multiscale sample entropy (WMMSE) to simulated signals with different degree of τ (time lag vector), M (embedding vector), r (threshold) and N (signal length) versus scale. The error bar at each scale indicates the entropy values which calculated 100 independent signals. (A) The results of MMSE and WMMSE on random series $N = 10{,}000$, $M = 2$, $r = 0.2$ with different τ are plotted versus scale. (B) The results of MMSE and WMMSE on random series $N = 10{,}000$, $M = 1$, $r = 0.2$ with different M are plotted versus scale. (C) The results of WMMSE on random series $N = 10{,}000$, $M = 2$, $\tau = 1$ with different r are plotted versus scale. (D) The results of MMSE and WMMSE on random series $M = 2$, $\tau = 1$, $r = 0.15$ with different N are plotted versus scale.

3. Results

3.1. Simulated signals

As a first motivation, to compare the performance of WMCMSE with those of MMSE, WMMSE and MCMSE, we apply the four methods to simulated signals with different degree of τ (time lag vector), M (embedding vector), r (threshold) and N (signal length). We construct 10,000 samples of white Gaussian noise with zero mean and unit variance. In each case, 100 independent samples are adopted in simulation. Regarding different τ and M, the entropy values obtained by using the MMSE, and WMMSE are nearly equal (see Fig. 2(A) and (B)). Fig. 2(C) shows that as r values increase from $r = 0.1$ to $r = 0.2$, the values of WMMSE gradually decrease. And WMMSE is able to distinguish among different r values. In Fig. 2(D), to quantitatively illustrate the effect of data lengths on the values of WMMSE algorithm, we perform the experiments of random series with data lengths $N = 1000$, 2000, 5000, 10,000, 20,000 and 50,000 respectively. The results indicate the entropy values obtained by applying WMMSE algorithm to random series with different data lengths are nearly equivalent. Generally, the results of WMMSE are relatively sensitive to parameter r.

As the next step, we present the entropy and standard deviation values of random series for the data length $N = 10{,}000$ in the M range [2, 2], the τ range [1, 1] and the r range 0.15 by using these four methods respectively in Fig. 3. There are 100 independent samples adopted in each simulation. As the scale factor increases, the entropy measures for all four methods decrease. The entropy values obtained by using those of four methods for random series are similar (see Fig. 3(A)). However, it is found that standard deviation curves of MCMSE and WMCMSE methods behave almost the same, and those of MMSE and WMMSE methods are similar. In addition, smaller standard deviation values of MCMSE and WMCMSE methods are assigned at all scales compared to those of MMSE and WMMSE methods in Fig. 3(B). In other words, the MCMSE and WMCMSE outperform the other two algorithms.

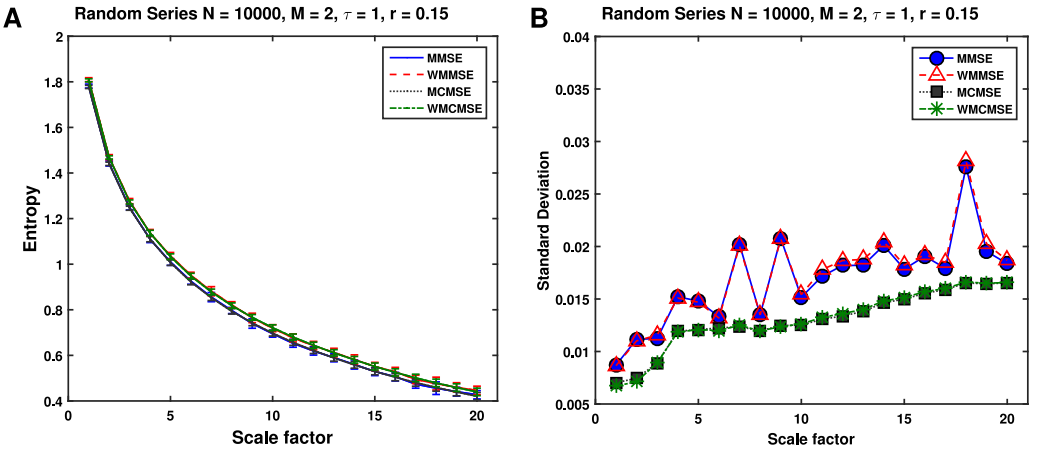

Fig. 3. The comparison of the values of the entropy and standard deviation among multivariate multiscale sample entropy (MMSE), weighted multivariate multiscale sample entropy (WMMSE), multivariate composite multiscale sample entropy (MCMSE) and weighted multivariate composite multiscale sample entropy (WMCMSE) on random series $N = 10{,}000$, $M = 2$, $\tau = 1$, $r = 0.15$ versus scale. There are 100 independent samples adopted in each simulation. (A) Entropy values by using MMSE, WMMSE, MCMSE and WMCMSE methods are plotted versus scale. (B) The standard deviations by using MMSE, WMMSE, MCMSE and WMCMSE methods are plotted versus scale.

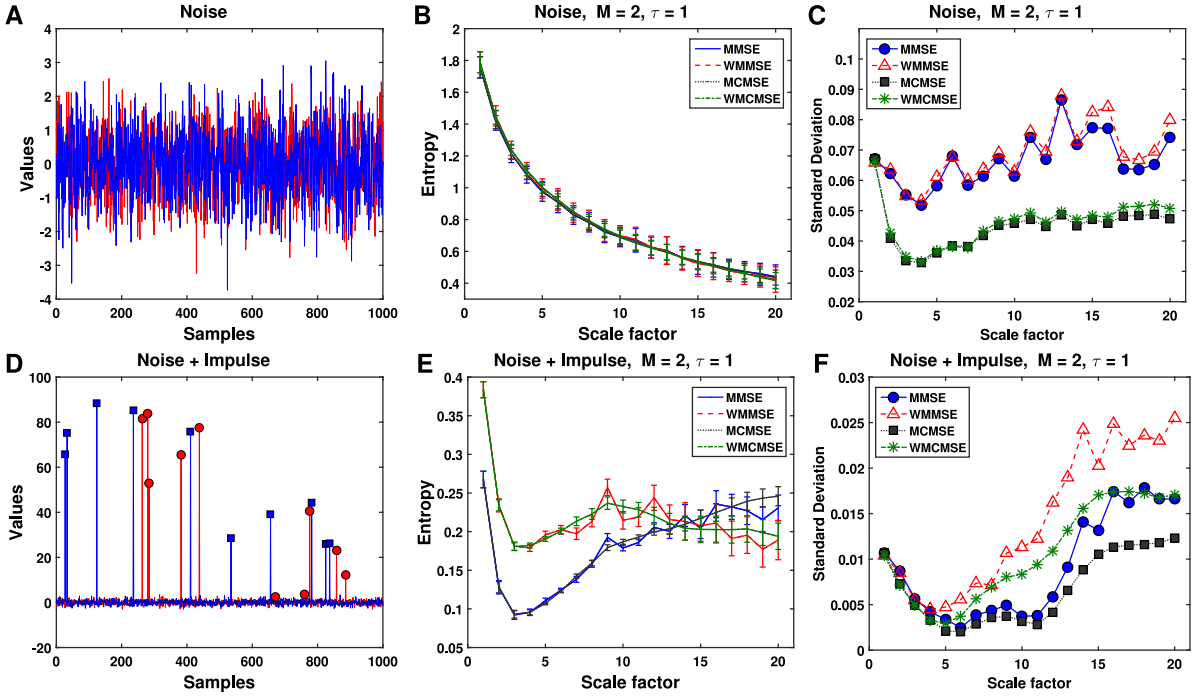

Fig. 4. The comparison of the values of the entropy and standard deviation between noise and noise plus impulse versus scale. (A) The values of two signals generated by Gaussian white noise with zero mean and unit variance with the length $N = 1000$. (B) Values of entropy acquired through MSE, WMMSE, MCMSE and WMCMSE computation using Gaussian white noise with different scale factors on 20 sets of 1000 successive signals. (C) Values of standard deviation acquired through MSE, WMMSE, MCMSE and WMCMSE computation using Gaussian white noise with different scale factors on 20 sets of 1000 successive signals. (D) The values of two signals consisting of an impulse and additive white Gaussian noise with zero mean and unit variance with the data length $N = 1000$. (E) Values of entropy acquired through MSE, WMMSE, MCMSE and WMCMSE computation using an impulse and additive white Gaussian noise with different scale factors on 20 sets of 1000 successive signals. (F) Values of standard deviation acquired through MSE, WMMSE, MCMSE and WMCMSE computation using an impulse and additive white Gaussian noise with different scale factors on 20 sets of 1000 successive signals.

Finally, we analyze the behavior of MMSE, WMMSE, MCMSE and WMCMSE in the presence of an impulsive and noisy signal. Impulse is some large fluctuation, in other words, adding some impulse in the noise will make the noise more fluctuate. Fig. 4(A) illustrates 1000 samples of two signals generated by Gaussian white noise with zero mean and unit variance, and Fig. 4(D) shows two signals consisting of an impulse and additive white Gaussian noise with zero mean and

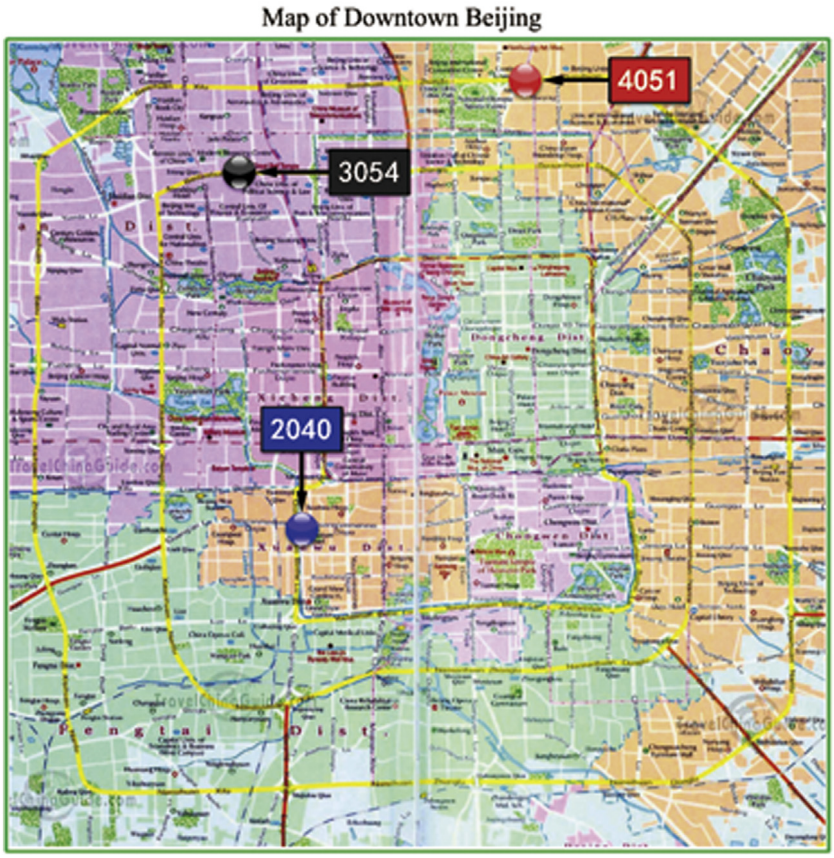

Fig. 5. The locations of detectors 2040, 3054, 4051.

unit variance with the data length $N = 1000$. The error bar at each scale indicates the values of the entropy and standard deviation which calculated 20 independent noise signals. Fig. 4(B) shows the entropy values of the WMCMSE are slightly less than those of the MMSE, WMMSE and MCMSE. And in Fig. 4(C), the standard deviation values of the MCMSE and WMCMSE are less than those of the MMSE and WMMSE. As shown in Fig. 4(E) and (F), because of impulse, the entropy and standard deviation values of WMCMSE is slightly higher than those of the three other methods. The weight is added to identify large fluctuations. The greater the entropy changes, the better the degree of recognition.

3.2. Traffic signals

Because the traffic data has a large fluctuation like simulation signals, WMCMSE is superior to other methods in dealing with traffic data. Therefore, the results of the other three methods applying to traffic time series are no longer presented. In this section, in order to illustrate the application of WMCMSE method, we employ it to explore the complexity of traffic time series. We get the data from the Highway Performance Measurement Project (HPMP) run by Beijing STONG Intelligent Transportation System Co. Ltd, Beijing, and use the traffic volume and speed time series observed from Detector 2040, 3054, 4051 which respectively lie on the 2nd, 3rd and 4th Ring Roads (Beijing, China) from August 11th to October 20th, 2012. Ring roads are highway systems in the city that serve as the backbones for the entire road traffic system. Ring 2 road are the inner circle surrounding the forbidden city as well as some key government and business areas. Therefore the Ring 2 road has the most severe traffic jam in all Ring roads. Ring 3, 4 roads approximately located concentrically with respect to Ring 2 road but are further away from the center. In general, the Ring 3 road has a better traffic flow compared to Ring 2 road and Ring 4 road has the best traffic flow. The main feature of traffic time series has three patterns: morning peak (from 7:00 to 9:00), evening peak (from 17:00 to 19:00) and idle time (0:00 to 02:00). The outer and inner rings are respectively traffic data on lane 1, 2, 3 and lane 11, 12, 13.

Fig. 5 shows the locations of the detectors. The left panel of Fig. 5 illustrates the traffic speed and volume time series on lanes 1, 2, and 3 collected by Detector 3057 on outer ring. The right panel of Fig. 6 shows those on inner ring.

Now, we turn to the analysis of traffic signals using WMCMSE method and show how new method reveals the intrinsic properties of traffic series. Firstly, we apply WMCMSE to make a distinction between outer and inner rings of those traffic

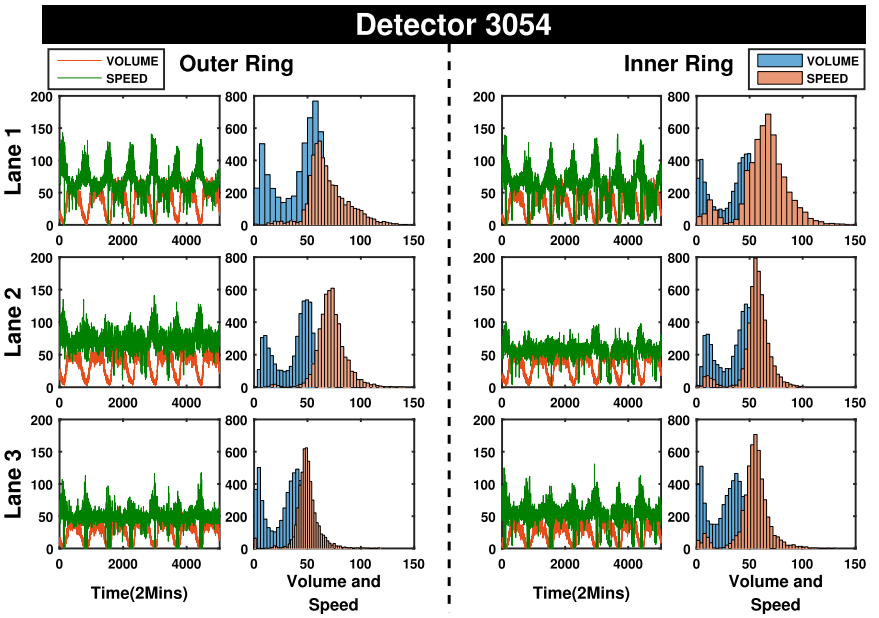

Fig. 6. Speed and volume series and distribution of outer ring collected by Detector 3054 from Aug. 18 to Aug. 25 (left panel) and Speed and volume series of inner ring collected by Detector 3054 from August 11th to October 20th, 2012 (right panel).

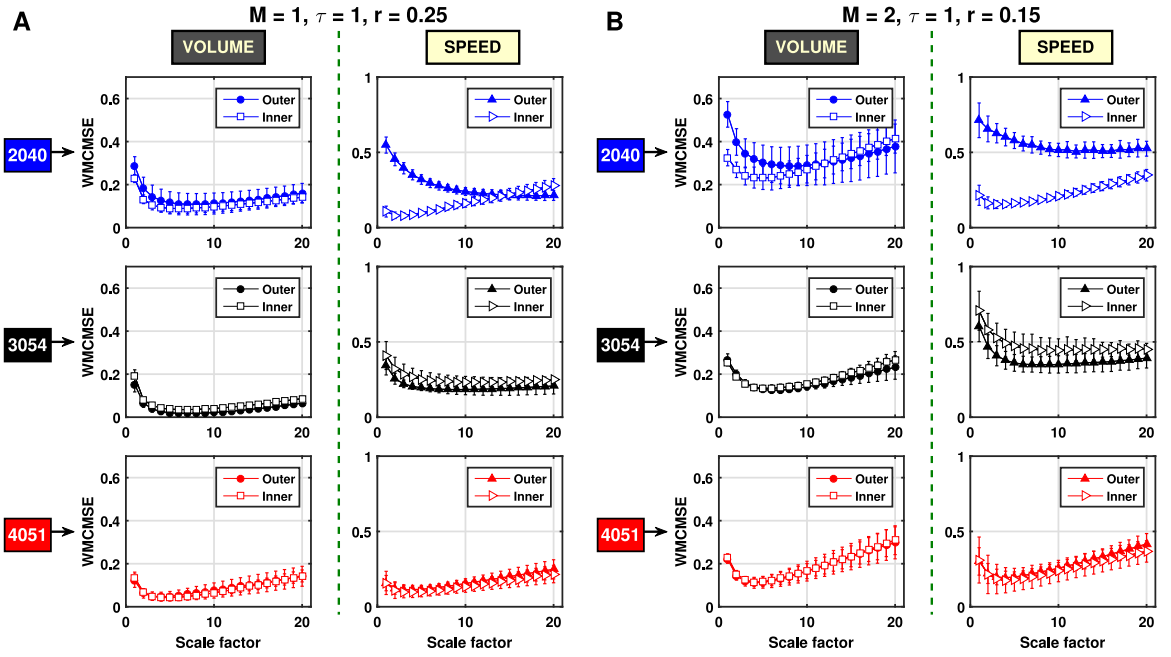

Fig. 7. The WMCMSE results for the volume and speed traffic series of detector 2040, 3054 and 4051 at different parameters for outer and inner rings versus scale. (A) The values of WMCMSE for the volume and speed traffic series of detector 2040, 3054 and 4051 under the fixed parameters $M = 1$, $\tau = 1$ and $r = 0.25$ are respectively plotted versus scale for outer and inner rings. (B) The values of WMCMSE for the volume and speed traffic series of detector 2040, 3054 and 4051 at $M = 2$, $\tau = 1$ and $r = 0.15$ are respectively plotted versus scale for outer and inner rings.

time series observed at different detectors and validate this kind of classification from the view of complexity in Fig. 7. The parameters of WMCMSE algorithm are set to $M = 1$, $\tau = 1$ and $r = 0.25$ in Fig. 7(A). After several experiments, we notice that the results of WMCMSE analysis are relatively better when the parameters are changed to $M = 2$, $\tau = 1$ and $r = 0.15$ than other cases. WMCMSE are calculated from scales 1 to 20. Compared to the volume time series of detectors 2040 and 3054, WMCMSE analysis on the speed time series of detectors 2040 and 3054 can distinguish outer and inner rings in Fig. 7(A). In particular, the WMCMSE obtained from the speed time series of detector 2040 drops dramatically with the

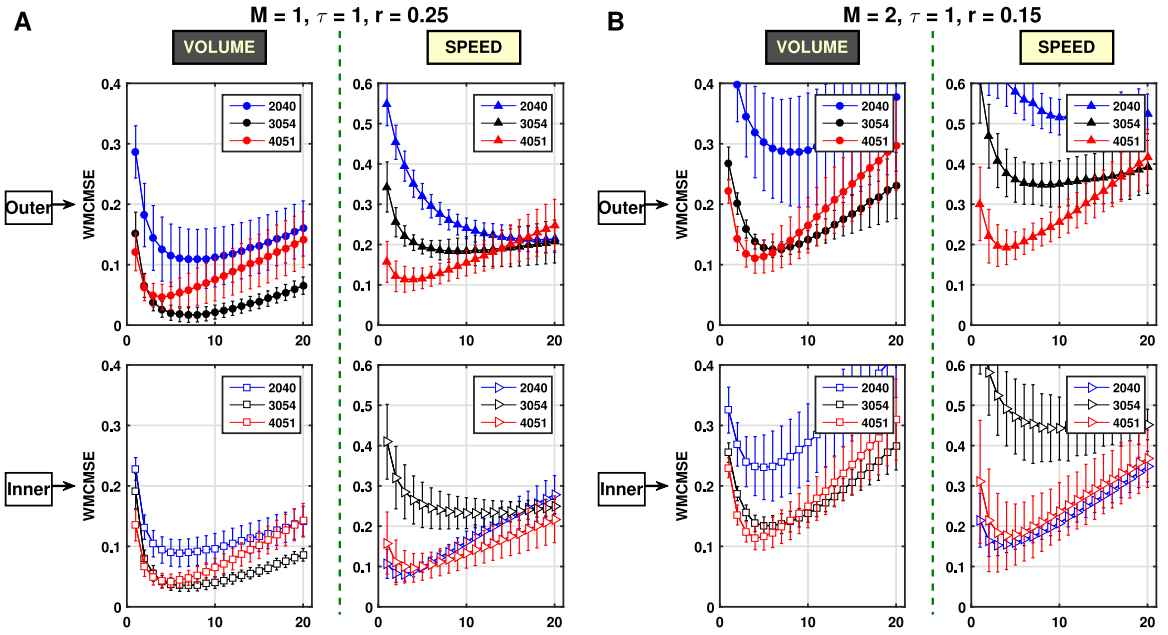

Fig. 8. The WMCMSE results for the volume and speed traffic series of outer and inner rings at different parameters for different parameters versus scale. (A) The values of WMCMSE for the volume and speed traffic series of outer and inner rings under the fixed parameters $M = 1$, $\tau = 1$ and $r = 0.25$ are respectively plotted versus scale for detector 2040, 3054 and 4051. (B) The values of WMCMSE for the volume and speed traffic series of outer and inner rings at $M = 2$, $\tau = 1$ and $r = 0.15$ are respectively plotted versus scale for detector 2040, 3054 and 4051.

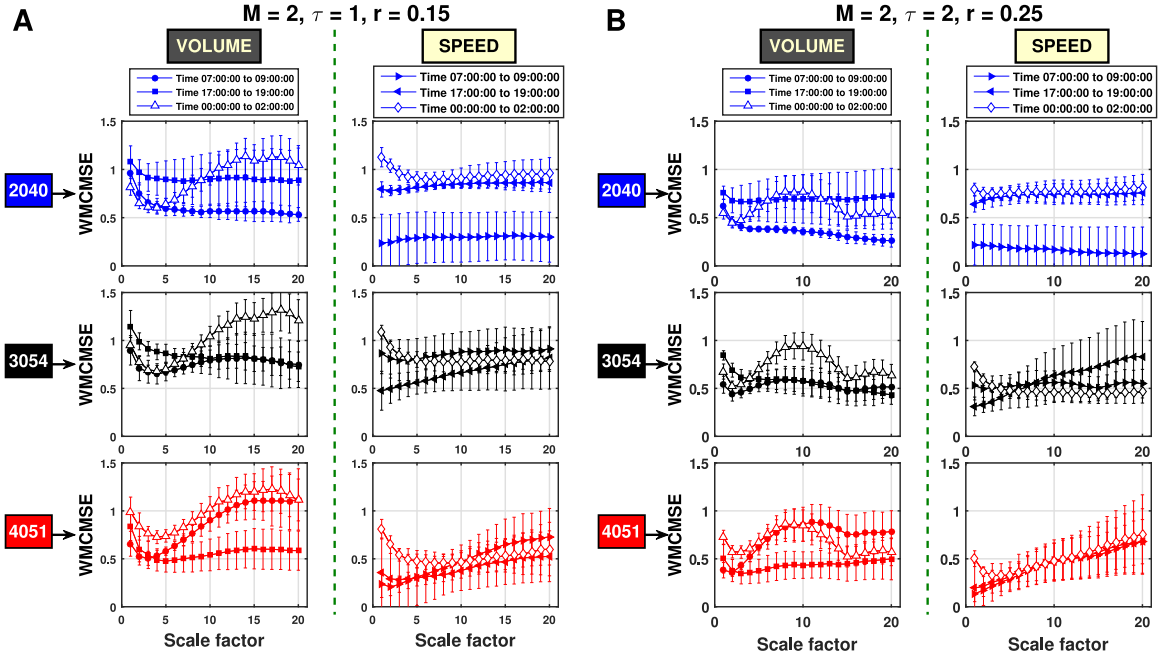

Fig. 9. The WMCMSE results for the volume and speed traffic series of detector 2040, 3054 and 4051 for different parameters versus scale. (A) The values of WMCMSE for the volume and speed traffic series of detector 2040, 3054 and 4051 under the fixed parameters $M = 1$, $\tau = 1$ and $r = 0.25$ are respectively plotted versus scale for time 07:00:00 to 09:00:00 (rush hours), time 17:00:00 to 19:00:00 (rush hours) and time 00:00:00 to 02:00:00 (idle time). (B) The values of WMCMSE for the volume and speed traffic series of detector 2040, 3054 and 4051 at $M = 2$, $\tau = 2$ and $r = 0.25$ are respectively plotted versus scale for time 07:00:00 to 09:00:00 (rush hours), time 17:00:00 to 19:00:00 (rush hours) and time 00:00:00 to 02:00:00 (idle time).

decrease of outer ring, while WMCMSE increases for inner ring in Fig. 7(A). From the bottom panel of Fig. 7(A), it is hard to identify outer and inner rings. There are some similarities between Fig. 7(A) and (B) except for the upper panel of Fig. 7. For the speed time series of detector 2040, it is notable that WMCMSE analysis can distinct outer and inner rings better when

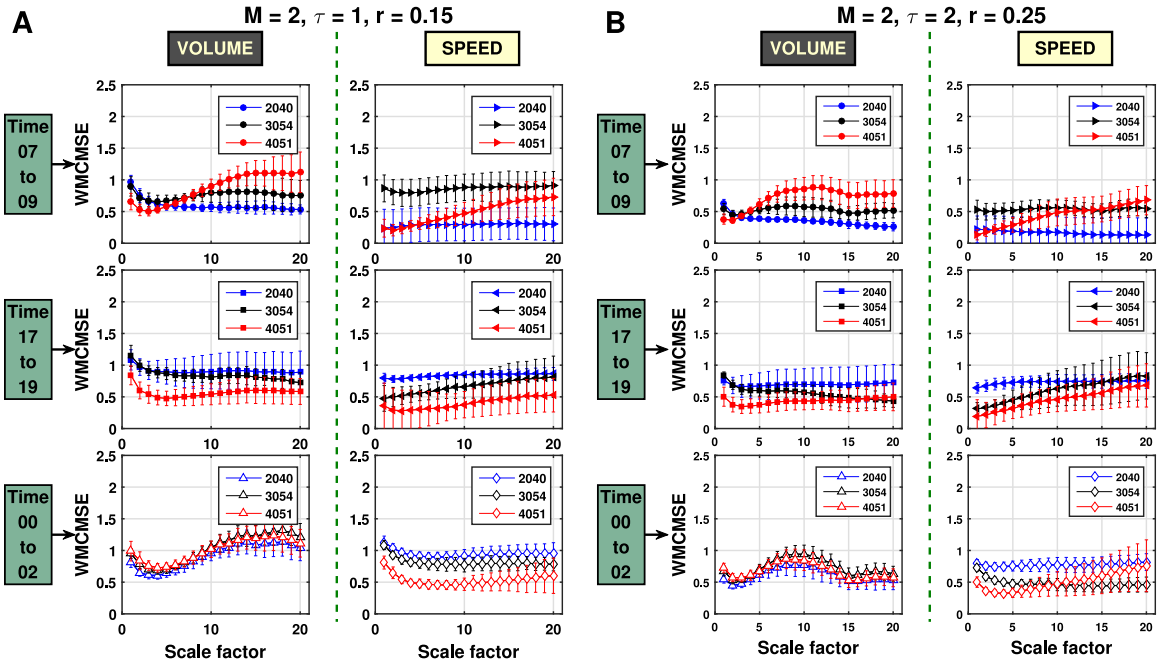

Fig. 10. The WMCMSE results for the volume and speed traffic series of three periods of time for different parameters versus scale. (A) The values of WMCMSE for the volume and speed traffic series of three periods of time are respectively under the fixed parameters $M = 2$, $\tau = 2$ and $r = 0.25$ plotted versus scale for detector 2040 (blue lines), 3054 (black lines) and 4051 (red lines). (B) The values of WMCMSE for the volume and speed traffic series of three periods of time at $M = 2$, $\tau = 2$ and $r = 0.25$ are respectively plotted versus scale for detector 2040, 3054 and 4051. (For interpretation of the references to colour in this figure legend, the reader is referred to the web version of this article.)

the parameters are set to $M = 2$, $\tau = 1$ and $r = 0.15$ than $M = 1$, $\tau = 1$ and $r = 0.25$. Generally, the complexity of 2nd Ring Road is highest, followed by 3rd and 4th Ring Roads. The complexity is reflection of the traffic congestion [10,42,43]. It is pointed out that the higher the complexity, the more traffic jams, which is relative in the above literature. The limits of traffic jams are also different according to the different circumstances. In other words, Beijing 2nd Ring Road has the worst traffic jams, 3rd Ring Road the second, 4th Ring Road the third [44].

Next, we show the results of WMCMSE analysis of traffic series based on different detectors. We take the speed and volume traffic series, and set $M = 1$, $\tau = 1$ and $r = 0.25$. From Fig. 8(A), we find the significant differences among 2040, 4051 and 3054 detectors. Whatever inner or outer rings, for volume series, the Ring 2 is the most complex system, the Ring 4 the second, the Ring 3 the third. For speed series of outer ring, the Ring 2 is the most complex system, followed by the Ring 3 and 4. For speed time series of inner ring, the Ring 3 is the most complex system, the next the Ring 2, the least the Ring 4. The obtained result of volume time series for $M = 2$, $\tau = 1$ and $r = 0.25$ is similar with left panel of Fig. 8. So we set the parameters $M = 2$, $\tau = 1$ and $r = 0.15$. And in Fig. 8(B) we find WMCMSE analysis on volume and speed time series of outer ring displays the similar trend to it in Fig. 8(A), while for volume and speed time series of inner ring in the bottom panel of Fig. 8(B), it is difficult to distinguish the differences of detector 3054 and detector 4051. From the above results, it can be observed that it helps us to further understand the traffic time series and their complexity at different scales.

Then, in Fig. 9, we show the results of the WMCMSE analysis of different periods of time according to different detectors, which are located on Beijing Ring 2, 3, 4 roads. With the parameters $M = 1$, $\tau = 1$ and $r = 0.25$, we give the WMCMSE plot in Fig. 9. The higher the entropy we get, the worse road condition will be. See the left of Fig. 9(A), for all volume time series at 0:00 to 02:00, has highest complexity. Further, for volume time series of 2nd Ring Road, the evening peak is more complex than the morning peak, which is consistent with the fact that the traffic of 2nd Ring Road at 17:00 to 19:00 is very heavy. Instead, for volume time series of 4th Ring Road, the morning peak is more complex than the evening peak, which is consistent with the fact that the traffic of 4th Ring Road at 7:00 to 9:00 is very heavy. For volume time series of 3rd Ring Road, it is difficult to distinguish the morning peak and evening peak. When we set $M = 2$, $\tau = 2$ and $r = 0.25$, it does not seem to change much while the complexity of volume time series at 0:00 to 02:00 has great changes. Fig. 9(B) shows similar results gained from WMCMSE. For speed time series of 2 road, the evening peak is more complex than the morning peak. And for speed time series of 3rd and 4th Ring Roads, the morning peak is more complex than the evening peak. It is observed that there is no significant difference between different parameters except for speed time series of 4th Ring Road, it fails to distinguish three periods of time.

Finally, for volume series during the morning peak, 4051 is the most complex system, the next 3054, the least 2040. The MMSE analysis is in line with our intuition that traffic congestion problem of 4th Ring Road in Beijing at 7:00 to 9:00 is

particularly acute [44]. On the contrary, for volume series during the morning peak, 2040 is the most complex system, 3054 the second, 4051 the third. This result is consistent with the fact that, 2nd Ring Road at 17:00 to 19:00 is the most congested ring. At 0:00 to 02:00, the roads of all rings have less traffic, so it cannot distinguish the complexity of three rings. When parameters are changed as $M = 2$, $\tau = 2$ and $r = 0.25$, the results are similar with the left panel of Fig. 10(A) shown as Fig. 10(B). The right panel of Fig. 10(A) depicts at 7:00 to 9:00 3054 is the most complex system, the next 4051, the least 2040, and at 17:00 to 19:00 and 0:00 to 02:00, 2040 is the most complex system, followed by 3054 and 4051. The results with $M = 2$, $\tau = 2$ and $r = 0.25$ displays the similar trend to the time scale except in the case of analysis for speed series at 0:00 to 02:00, which fails to distinguish 3rd and 4th Ring Roads.

The above results help us to further understand the traffic condition and their complexity at different scales. In addition, those results give us a suggestion that when predict the traffic time series of the inner and outer rings should be treated differently for example.

4. Conclusions

In this paper, weighted multivariate composite multiscale sample entropy (WMCMSE) is proposed to measure the complexity of traffic time series of Beijing. The necessity and advantage of WMCMSE are shown by comparing WMCMSE results with the multivariate multiscale sample entropy (MMSE), weighted multivariate multiscale sample entropy (WMMSE), multivariate composite multiscale sample entropy (MCMSE) results on random series, respectively. The simulation results demonstrate that WMCMSE is capable of accurately reflecting the complexity of signals. We apply WMCMSE to study the multichannel data in the traffic system directly and detect much richer information contained in the traffic time series. The results have clearly shown that WMCMSE method is able to distinguish traffic time series behavior, which means we can detect congestion of traffic system. We find the behaviors of Ring 2, 3, 4 road conditions are quite different. Compared with 4th Ring Road, 2nd and 3rd Ring Roads series presents the higher values, indicating 2nd and 3rd Ring Roads are more complex. Since the similarity of people behaviors in the same period of time, the behaviors of Ring 2, 3, 4 road at different times are also different. Those observations support that Beijing has a large population and the complicated traffic situation [13]. In addition, WMCMSE method can be also used as a sorting technique. While WMCMSE can provide more accurate information concerning the complexity of traffic signals for better understanding the dynamics and inner mechanism of traffic system, further related work is required to study the traffic congestion evaluation index systems, such as developing a new traffic congestion levels.

Finally, it is worth noting for further use of WMCMSE method to different types of time series [24,26,45]. Especially for the physiologic signals, the WMCMSE can be useful in the context of network physiology. Because some recent work [46–48] has demonstrated that physiologic interaction carries important information about the underlying regulatory mechanisms. In particular, research on network physiology has demonstrated that complex integrated physiologic functions can be understood via advanced time series analysis methodology. Therefore, it is reasonable to speculate a board application of the proposed WMCMSE approach as it might capture the complexity of time series of pairwise physiologic coupling strength. Also, changes in the complexity of the output signals are often associated with changes in the physiologic function and transition across physiologic states, therefore, WMCMSE might serve as new hallmarks of physiologic states and functions.

Acknowledgments

This work is supported by the National Natural Science Foundation of China (Grant no. 61673005 and 61771035) and the Fundamental Research Funds for the Central Universities of China (Grant no. 20170081008).

References

[1] B. Toledo, M. Sanjuan, V. Munoz, J. Rogan, J. Valdivia, Non-smooth transitions in a simple city traffic model analyzed through supertracks, Commun. Nonlinear Sci. Numer. Simul. 18 (1) (2013) 81–88.
[2] L. Yu, Z. Shi, B. Zhou, Kink–antikink density wave of an extended car-following model in a cooperative driving system, Commun. Nonlinear Sci. Numer. Simul. 13 (10) (2008) 2167–2176.
[3] S.V. George, G. Ambika, R. Misra, Detecting dynamical states from noisy time series using bicoherence, Nonlinear Dynam. (2017) 1–15.
[4] H. Zhang, J. Liu, D. Ma, Z. Wang, Data-core-based fuzzy min–max neural network for pattern classification, IEEE Trans. Neural Netw. 22 (12) (2011) 2339–2352.
[5] P.D. Domański, M. Ławryńczuk, Assessment of predictive control performance using fractal measures, Nonlinear Dynam. 89 (2) (2017) 773–790.
[6] W. Leutzbach, Introduction to the Theory of Traffic Flow, vol. 47, Springer, 1988.
[7] B.S. Kerner, The physics of traffic, Phys. World 12 (8) (1999) 25.
[8] D. Chowdhury, L. Santen, A. Schadschneider, Statistical physics of vehicular traffic and some related systems, Phys. Rep. 329 (4) (2000) 199–329.
[9] D. Helbing, Traffic and related self-driven many-particle systems, Rev. Modern Phys. 73 (4) (2001) 1067.
[10] Z.-y. Gao, J.-j. Wu, B.-h. Mao, H.-j. Huang, Study on the complexity of traffic networks and related problems, Commun. Trans. Syst. Eng. Inf. 2 (2005) 014.
[11] Y. Yin, P. Shang, Multivariate multiscale sample entropy of traffic time series, Nonlinear Dynam. 86 (1) (2016) 479–488.
[12] M. Xu, P. Shang, J. Xia, Traffic signals analysis using qsdiff and qhdiff with surrogate data, Commun. Nonlinear Sci. Numer. Simul. 28 (1) (2015) 98–108.
[13] J. Wang, P. Shang, X. Zhao, J. Xia, Multiscale entropy analysis of traffic time series, Internat. J. Modern Phys. C 24 (02) (2013) 1350006.
[14] X. Wang, P. Shang, J. Fang, Traffic time series analysis by using multiscale time irreversibility and entropy, Chaos 24 (3) (2014) 032102.
[15] Y. Yin, P. Shang, Multifractal cross-correlation analysis of traffic time series based on large deviation estimates, Nonlinear Dynam. 81 (4) (2015) 1779–1794.

[16] J. Wang, P. Shang, X. Cui, Multiscale multifractal analysis of traffic signals to uncover richer structures, Phys. Rev. E 89 (3) (2014) 032916.
[17] P. Shang, Y. Lu, S. Kamae, Detecting long-range correlations of traffic time series with multifractal detrended fluctuation analysis, Chaos Solitons Fractals 36 (1) (2008) 82–90.
[18] P. Shang, X. Li, S. Kamae, Chaotic analysis of traffic time series, Chaos Solitons Fractals 25 (1) (2005) 121–128.
[19] P. Shang, X. Li, S. Kamae, Nonlinear analysis of traffic time series at different temporal scales, Phys. Lett. A 357 (4) (2006) 314–318.
[20] M. Costa, A.L. Goldberger, C.-K. Peng, Multiscale entropy analysis of complex physiologic time series, Phys. Rev. Lett. 89 (6) (2002) 068102.
[21] M. Costa, C.-K. Peng, A.L. Goldberger, J.M. Hausdorff, Multiscale entropy analysis of human gait dynamics, Physica A 330 (1) (2003) 53–60.
[22] M. Costa, A.L. Goldberger, C.-K. Peng, Multiscale entropy analysis of biological signals, Phys. Rev. E 71 (2) (2005) 021906.
[23] A. Humeau-Heurtier, The multiscale entropy algorithm and its variants: A review, Entropy 17 (5) (2015) 3110–3123.
[24] M.U. Ahmed, D.P. Mandic, Multivariate multiscale entropy analysis, IEEE Signal Process. Lett. 19 (2) (2012) 91–94.
[25] D. Looney, M.U. Ahmed, D.P. Mandic, Human-centred multivariate complexity analysis, Nat. Intel. 1 (3) (2012) 40–43.
[26] D. Labate, F. La Foresta, G. Morabito, I. Palamara, F.C. Morabito, Entropic measures of eeg complexity in alzheimer's disease through a multivariate multiscale approach, IEEE Sens. J. 13 (9) (2013) 3284–3292.
[27] Z.-K. Gao, Y.-X. Yang, P.-C. Fang, Y. Zou, C.-Y. Xia, M. Du, Multiscale complex network for analyzing experimental multivariate time series, Europhys. Lett. 109 (3) (2015) 30005.
[28] Z.-K. Gao, M.-S. Ding, H. Geng, N.-D. Jin, Multivariate multiscale entropy analysis of horizonta l oil–water two-phase flow, Physica A 417 (2015) 7–17.
[29] Q. Wei, D.-H. Liu, K.-H. Wang, Q. Liu, M.F. Abbod, B.C. Jiang, K.-P. Chen, C. Wu, J.-S. Shieh, Multivariate multiscale entropy applied to center of pressure signals analysis: an effect of vibration stimulation of shoes, Entropy 14 (11) (2012) 2157–2172.
[30] C.-W. Huang, P.-D. Sue, M.F. Abbod, B.C. Jiang, J.-S. Shieh, Measuring center of pressure signals to quantify human balance using multivariate multiscale entropy by designing a force platform, Sensors 13 (8) (2013) 10151–10166.
[31] A. Humeau-Heurtier, C.-W. Wu, S.-D. Wu, Refined composite multiscale permutation entropy to overcome multiscale permutation entropy length dependence, IEEE Signal Process. Lett. 22 (12) (2015) 2364–2367.
[32] S.-D. Wu, C.-W. Wu, S.-G. Lin, K.-Y. Lee, C.-K. Peng, Analysis of complex time series using refined composite multiscale entropy, Phys. Lett. A 378 (20) (2014) 1369–1374.
[33] J. Wang, P. Shang, J. Xia, W. Shi, Emd based refined composite multiscale entropy analysis of complex signals, Physica A 421 (2015) 583–593.
[34] S.-D. Wu, C.-W. Wu, S.-G. Lin, C.-C. Wang, K.-Y. Lee, Time series analysis using composite multiscale entropy, Entropy 15 (3) (2013) 1069–1084.
[35] J. Xia, P. Shang, J. Wang, W. Shi, Permutation and weighted-permutation entropy analysis for the complexity of nonlinear time series, Commun. Nonlinear Sci. Numer. Simul. 31 (1) (2016) 60–68.
[36] X. Chen, N.-D. Jin, A. Zhao, Z.-K. Gao, L.-S. Zhai, B. Sun, The experimental signals analysis for bubbly oil-in-water flow using multi-scale weighted-permutation entropy, Physica A 417 (2015) 230–244.
[37] B. Deng, L. Liang, S. Li, R. Wang, H. Yu, J. Wang, X. Wei, Complexity extraction of electroencephalograms in alzheimer's disease with weighted-permutation entropy, Chaos 25 (4) (2015) 043105.
[38] B. Fadlallah, B. Chen, A. Keil, J. Príncipe, Weighted-permutation entropy: A complexity measure for time series incorporating amplitude information, Phys. Rev. E 87 (2) (2013) 022911.
[39] Y. Yin, P. Shang, Weighted permutation entropy based on different symbolic approaches for financial time series, Physica A 443 (2016) 137–148.
[40] J.P. Toomey, D.M. Kane, T. Ackemann, Complexity in pulsed nonlinear laser systems interrogated by permutation entropy, Opt. Express 22 (15) (2014) 17840–17853.
[41] J.S. Richman, J.R. Moorman, Physiological time-series analysis using approximate entropy and sample entropy, Am. J. Physiol.-Heart C. Physiol. 278 (6) (2000) H2039–H2049.
[42] B.S. Kerner, H. Rehborn, Experimental properties of complexity in traffic flow, Phys. Rev. E 53 (5) (1996) R4275.
[43] X.-G. Li, Z.-Y. Gao, K.-P. Li, X.-M. Zhao, Relationship between microscopic dynamics in traffic flow and complexity in networks, Phys. Rev. E 76 (1) (2007) 016110.
[44] X. Chen, X. Xia, Y. Zhao, P. Zhang, Heavy metal concentrations in roadside soils and correlation with urban traffic in Beijing, China, J. Hazard. Mater. 181 (1) (2010) 640–646.
[45] M.U. Ahmed, D.P. Mandic, Multivariate multiscale entropy: A tool for complexity analysis of multichannel data, Phys. Rev. E 84 (6) (2011) 061918.
[46] R.P. Bartsch, K.K. Liu, A. Bashan, P.C. Ivanov, Network physiology: how organ systems dynamically interact, PLoS One 10 (11) (2015) e0142143.
[47] P.C. Ivanov, K.K. Liu, A. Lin, R.P. Bartsch, Network physiology: From neural plasticity to organ network interactions, in: Emergent Complexity from Nonlinearity, in: Physics, Engineering and the Life Sciences, Springer, 2017, pp. 145–165.
[48] K.K. Liu, R.P. Bartsch, A. Lin, R.N. Mantegna, P.C. Ivanov, Plasticity of brain wave network interactions and evolution across physiologic states, Front. Neural Circuits 9 (2015).